Heliyon 10 (2024) e38584

Contents lists available at ScienceDirect

Heliyon

journal homepage: www.cell.com/heliyon

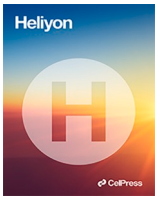

Research article

SS-31 modification alleviates ferroptosis induced by superparamagnetic iron oxide nanoparticles in hypoxia/reoxygenation cardiomyocytes

Qizheng Lu [a,1], Xiaobo Yao [b,1], Hao Zheng [c,1], Jinbo Ou [d], Jieyun You [d], Qi Zhang [d], Wei Guo [d], Jing Xu [d], Li Geng [d], Qinghua Liu [e], Ning Pei [f], Yongyong Gong [f], Hongming Zhu [g], Yunli Shen [d,*]

[a] *Department of Digestive Medicine, The Affiliated Guangdong Second Provincial General Hospital of Jinan University, Guangzhou, 510000, Guangdong Province, China*
[b] *Department of Cardiology, Punan Branch of Renji Hospital, Shanghai Jiaotong University School of Medicine, Shanghai, 200125, China*
[c] *Department of Critical Care Medicine, Zhongda Hospital, School of Medicine, Southeast University, Nanjing, 210009, China*
[d] *Department of Cardiology, Shanghai East Hospital, Tongji University School of Medicine, Shanghai, 200120, China*
[e] *Department of Pulmonary and Critical Care Medicine, Shanghai East Hospital, Tongji University School of Medicine, Shanghai, 200120, China*
[f] *College of Science, Shanghai University, Shanghai, 200444, China*
[g] *Translational Medical Center for Stem Cell Therapy, Institute for Regenerative Medicine, Shanghai East Hospital, Tongji University School of Medicine, Shanghai, 200120, China*

ARTICLE INFO

Keywords:
Superparamagnetic iron oxide nanoparticles (SPION)
SS-31
Ferroptosis
Cardiotoxicity
Mitochondria

ABSTRACT

Superparamagnetic iron oxide nanoparticles (SPION) are widely used in cardiovascular applications. However, their potential to induce ferroptosis in myocardial cells post-ischemia-reperfusion hinders clinical adoption. We investigated the mechanisms behind SPION-induced cytotoxicity in myocardial cells and explored whether co-loading SPION with SS-31 (a kind of mitochondrial-targeted antioxidant peptide) could counteract this toxicity.

To create SPION@SS-31, SS-31 was physically adsorbed onto SPION. To study the dose- and time-dependent cytotoxic effects and assess the influence of SS-31 on reducing SPION-induced damage, hypoxia/reoxygenation(H/R) H9C2 cells were treated with either SPION or SPION@SS-31. We examined the relationship between SPION and ferroptosis by measuring mitochondrial ROS, mitochondrial membrane potential (MMP), lipid peroxidation products, ATP, GSH, GPX4, mitochondrial structure, nonheme iron content, cellular iron regulation, and typical ferroptosis markers.

The findings showed that SPION induced concentration- and time-dependent toxicity, marked by a significant cell viability loss and an increase in LDH levels. In contrast, SPION@SS-31 produced results comparable to the H/R group, implying that SS-31 can notably reduce cell damage induced by SPION. SPION disrupted cellular iron homeostasis, with FtH and FtMt expression increased and reduced levels of FPN1 and ABCB8, which led to the overload of mitochondrial iron. This iron dysregulation damaged mitochondrial function and integrity, causing ATP depletion, MMP loss, and decreased GPX4 and GSH levels, accompanied by a burst of mitochondrial lipid peroxidation, ultimately resulting in ferroptosis in H/R cardiomyocytes. Notably,

* Corresponding author.
E-mail address: shenyunli2011@163.com (Y. Shen).
[1] These authors contributed equally to this work and share first authorship.

https://doi.org/10.1016/j.heliyon.2024.e38584
Received 12 June 2024; Received in revised form 25 September 2024; Accepted 26 September 2024
Available online 27 September 2024

SS-31 significantly alleviated SPION-induced ferroptosis by decreasing mitochondrial MDA production and maintaining GSH and GPX4 levels, indicating its possibility to reverse SPION-induced cytotoxicity. The viability of H/R cells and cells treated with SPION and Fer-1 did not differ statistically, whereas cells exposed to SPION along with inhibitors like 3-MA, zVAD, or Nec-1 showed a substantial loss in viability, implying that ferroptosis is the primary mechanism behind SPION-induced myocardial toxicity.

SPION triggers mitochondrial lipid peroxidation by causing overload of iron, leading to ferroptosis in H/R H9C2 cells. Mitochondria appear to be the primary target of SPION-induced toxic effects. SS-31 demonstrates potential in inhibiting this ferroptosis by acting as a mitochondria-targeted antioxidant, suggesting that the modification of mitochondria-targeted antioxidant peptides represents an innovative and practical approach to attenuate the myocardial toxicity associated with SPION.

1. Introduction

Cardiomyopathy iron-overload is one of the primary factor in morbidity and mortality in primary hemochromatosis patients and plays a crucial part in the survival of patients with secondary overload of iron [1], indicating that metabolically active cardiomyocytes are quite sensitive to the toxicity of iron overload. In two decades, SPION have been widely used in cardiovascular diagnostics and therapies, serving as MR contrast agents [2], cell tracers [3], and carriers for magnetic-targeted therapy [4,5] implying that superparamagnetic iron oxide nanoparticles have a lot of potentials in the cardiovascular field. However, SPION have been found to induce toxicity to normal myocardium after intravenous injection [6], and myocardial injury is more serious following repeated intraperitoneal injection [7]. Our previous study revealed that the oxidative stress damage of SPION-induced cardiomyocytes after the hypoxia/reoxygenation (H/R) procedure was significantly greater than that of normal cardiomyocytes [8], suggesting that ischemic myocardium may be more vulnerable than normal myocardium. The myocardial toxicity of SPIONs poses a challenge to their clinical application. Despite this, the molecular mechanisms underlying SPION-induced ischemic myocardial toxicity remain unclear. Therefore, elucidating these mechanisms is crucial to enhancing the safety of SPION.

Recently, growing evidence has suggested that the Ferroptosis is related to I/R injury closely [9]; subsequently, Ferroptosis is regarded as a new target treating I/R injury [10]. Ferroptosis was found to be involved in ventricular remodeling and fibrosis following myocardial ischemia-reperfusion in mice, in which mitochondria are important organelles determining myocardial Ferroptosis [11].

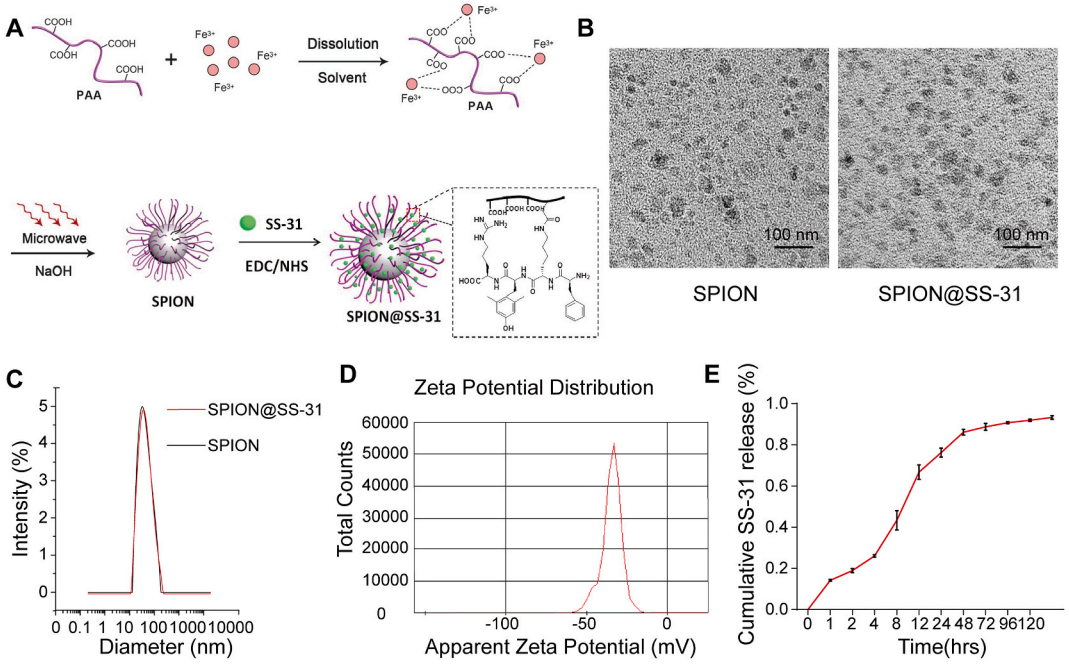

Fig. 1. Characterization of SPION@SS-31. (A) Schematic diagram of SPION@SS-31 synthesis. (B) Representative TEM images of SPION and SPION@SS-31. (C) Hydrodynamic diameter distribution of SPION@SS-31 in PBS. (D) Zeta potential distribution of SPION@SS-31. (E) Profile of SS-31 release from the SPION@SS-31 dissolved in PBS (pH = 7.4) at 37 °C. Data were collected from three independent experiments.
Abbreviations: SPION, superparamagnetic iron oxide nanoparticles; SPION@SS-31, SPION modified with SS-31; TEM, transmission electron microscopy.

SPION have been proven to facilitate Ferroptosis of tumor cells by accelerating the Fenton reaction to produce lots of reactive oxygen species (ROS) [12,13], which is expected to be a crucial strategy in the treatment of carcinoma [14]. We speculated that SPION, when applied in ischemia-reperfusion myocardium, may aggravate Ferroptosis in ischemic cardiomyocytes by increasing the cardiomyocyte iron load [15]. As mitochondria are not only areas of reactive oxygen species (ROS) production but also the main organelles targeted by ROS, it is plausible that mitochondria are the key targets of SPION [15,16]. Previous research have demonstrated that the mitochondrial-targeted antioxidant peptides could effectively offer protection to mitochondria to rescue ischemia-reperfusion injury [17–19]. Based on the above, we make assumptions that SPION modified with mitochondrial-targeted antioxidant peptides could alleviate SPION-induced myocardial toxicity significantly. In this study, we employed SS-31, a potent mitochondrial targeting peptide [18,20], to modify SPION and assess its ability to alleviate SPION-induced adverse effects in vitro.

2. Materials and methods

2.1. SPION and SPION@SS-31 synthesis and preparation

A schematic representation is provided in Fig. 1A. SPION were synthesized via a microwave-assisted polyol process [21]. The collected SPION underwent washing, sterilization by filtration, and were suspended in sterile water (20 mg/mL). Next, 10 mg PEI 1600 (Adamas-beta) and 5 mg SS-31 (All Peptide) were added to sterile water (1 mL) and stirred for 60 min to form the SS-31@ PEI 1600 mixture. The SPION and SS-31@ PEI 1600 were then mixed and reacted for 120 min. Following washing and removal of unbound SS-31 through ultrafiltration (Millipore), the final product, SPION@SS-31, was obtained.

2.2. SPION@SS-31 characterization

The zeta potential and hydrodynamic diameters of SPION@SS-31 were measured using dynamic light scattering (DLS) at 298 K with the Zeta Sizer Nano (Malvern). Morphological analysis of SPION@SS-31 was performed using transmission electron microscopy (TEM) with a 200-kV acceleration voltage. 10 mg SPION@SS-31 placed inside a 10-kDa dialysis bag, and SS-31 concentrations were measured at 37 °C at different time intervals using the bicinchoninic acid assay on a spectrophotometer (NanoDrop1000, Thermo Scientific). The release of SS-31 was calculated, and cumulative release profiles were plotted against time.

2.3. Culture and the H/R procedure of primary rat cardiomyocytes and H9C2 cells

The primary cardiomyocytes from rats (obtained from the Shanghai Animal Administration Center) aged 1–3 days were isolated and cultured based on established methods [22]. Before the H/R procedure, cells were cultured for at least 3 days. All animal experiments adhered to the guidelines of the Animal Care and Use Committee of Tongji University.

H9C2 cells (Cell Bank, the Chinese Academy of Sciences, Shanghai Cat.No. GNR 5; RRID: CVCL_0286) from embryonic rat heart were cultured in DMEM containing FBS (10 %), penicillin (100 U/mL), and streptomycin (100 μg/mL) at 37 °C in a humidified incubator (Thermo Fisher Scientific, USA) with 95 % air and 5 % CO2. To simulate cardiomyocytes H/R injury, when cells reached 70–80 % confluence, they were placed at 37 °C with 5 % CO_2 and 95 % N_2 environment for 3 h in a hypoxic chamber (STEMCELL Technologies), succeeded by reoxygenation with 5 % CO_2 and 95 % normal air for 3 h as described earlier [8]. All assays were conducted using low cell passage (2–5 passages) cells.

2.4. Different nanoparticle treatments

To evaluate the effect of SPION or SPION@SS-31 concentrations on cell viability, H/R cardiomyocytes were treated with various concentrations of SPION (Fe_3O_4 range from 25 to 200 μg/mL) or SPION@SS-31 (Fe_3O_4 range from 25 to 200 μg/mL and SS-31 range from 7.91 to 31.64 μg/mL) for 1 day. To evaluate the effect of exposure duration on cytotoxicity, H/R cardiomyocytes were exposed to SPION (Fe_3O_4, 50 μg/mL) or SPION@SS-31 (Fe_3O_4, 50 μg/mL; SS-31, 15.82 μg/mL) for 24, 48, and 72 h post-H/R. To determine whether ferroptosis was the primary mode of SPION-induced cell death, H/R cardiomyocytes in 96-well plates were treated with SPION, SPION@SS-31, SPION+3-MA (Cat# S2767, Selleck Chemicals, 5 μM), SPION + Nec-1 (Cat# S8037, Selleck Chemicals, 5 μM), SPION + zVAD (Cat# 627610, Sigma-Aldrich, 5 μM) and SPION + Fer-1 (Cat# S7243, Selleck Chemicals, 5 μM) for 24 h.

2.5. Measurement of mitochondrial ROS and MMP

MitoSOX staining (Invitrogen, China) was performed to measure mitochondrial ROS after H9C2 cells were coincubated with SPION (Fe_3O_4 50 μg/mL) or SPION@SS-31 (including Fe_3O_4 50 μg/mL and SS-31 15.82 μg/mL) for 24 h. Cells were incubated with 5 μM MitoSOX at 37 °C for 10 min, and the fluorescence images were immediately captured using red channels. The mitochondrial membrane potential (MMP) in H9C2 cells co-incubated with SPION (Fe_3O_4 50 μg/mL) or SPION@SS-31 (including Fe_3O_4 50 μg/mL and SS-31 15.82 μg/mL) was evaluated using the JC-1 dye. After staining with 5 mmol/L JC-1 for 30 min at 37 °C, cells were resuspended and taken fluorescence images. Red/green fluorescence intensity ratios were calculated using Image J (V. 1.45).

2.6. Morphology of mitochondria

TEM (JEM 2010, JEOL) was used to observe morphological changes in mitochondria in H/R cardiomyocytes following incubation with SPION (Fe_3O_4 50 μg/mL) or SPION@SS-31 (including Fe_3O_4 50 μg/mL and SS-31 15.82 μg/mL) for 24 h.

2.7. Determination of cytotoxicity

LDH activity and Cell viability were evaluated using LDH assay kits and CCK-8 kit (Nanjing Jiancheng Bioengineering Institute) as described previously [8]. The H9C2 cells were used in LDH activity test while H9C2 cells and primary rat cardiomyocytes in cell viability test. The assays were performed according to the manufacturers' protocols, and optical densities were measured at 450 nm.

2.8. Detection of iron metabolism-related proteins and ferroptosis markers by western blot

After 24 h of SPION (Fe_3O_4 50 μg/mL) or SPION@SS-31 (including Fe_3O_4 50 μg/mL and SS-31 15.82 μg/mL) treatment, Western blotting (WB) was conducted based on previously described methods [23] with some modifications. Protein samples (30 mg) were transferred onto a nitrocellulose membrane after being resolved by 10–12 % SDS-PAGE, blocked with BSA (5 %) and subsequently incubated with primary antibodies, including anti-ferritin H (FTH) (Cat#GTX10173, GeneTex), anti-transferrin receptor 1 (TfR1) (Abcam), anti-ferroportin1 (FPN1) (Abcam), anti-ATP binding cassette protein B8 (ABCB8) (GeneTex), anti-nuclear erythroid Factor 2 (NRF2) (GeneTex), anti-glutathione peroxidase 4 (GPX4) (GeneTex), and anti-long-chain acyl-CoA synthetase (ACSL4) (Abcam), at a 1,000 dilution. Anti-β-actin (Millipore) was used at a 1:10,000 dilution. Visualization of protein bands was carried out using a Versa Doc Imaging System (Bio-Rad), and the densitometric analysis was performed using UN-SCAN-IT (Silk Scientific Corporation) software.

2.9. Detection of cytoplasmic and mitochondrial nonheme iron

Mitochondria were isolated from H9C2 cells treated with SPION (Fe_3O_4 50 μg/mL) or SPION@SS-31 (comprising Fe_3O_4 50 μg/mL and SS-31 15.82 μg/mL). The nonheme iron content in the cytoplasm and mitochondria was measured using the inductively coupled plasma mass spectrometry (ICP-MS), following previously published protocols [24].

2.10. Measurement of MDA, GPX4, GSH, ATP and FtMt

The malonaldehyde (MDA), glutathione peroxidase 4 (GPX4), glutathione (GSH), and adenosine triphosphate (ATP) levels in H/R cardiomyocytes treated with SPION (Fe_3O_4 50 μg/mL) or SPION@SS-31 (comprising Fe_3O_4 50 μg/mL and SS-31 15.82 μg/mL) were determined using ELISA kits (Cayman Chemicals) according to the manufacturer's instructions. Mitochondrial ferritin (FtMt) was measured using an ELISA kit from Shanghai BIOESN Biotechnology.

2.11. QPCR

After treatment with SPION (Fe_3O_4 50 μg/mL) or SPION@SS-31 (including Fe_3O_4 50 μg/mL and SS-31 15.82 μg/mL), RNA was extracted from H9C2 cells using TRIzol reagent (Ambion, USA). cDNA was synthesized with the Verso™ cDNA Kit (Thermo) from of total RNA (3 μg). QPCR was conducted with the LightCycler 480 System (Roche, Switzerland), and gene expression was analyzed according to the $2-\Delta\Delta Ct$ method relative to the Gapdh levels, as described previously [25].

2.12. Statistical analysis

Data were presented as means ± SD and analyzed using one-way ANOVA followed by the least significant difference (LSD) test. Statistical significance was set at $p < 0.05$, and analysis was performed using SPSS version 24.0 (SPSS, Chicago).

3. Results

3.1. SPION@SS-31 characterization

Both SPION and SPION@SS-31 exhibited a Fe_3O_4 single-crystal structure under TEM (Fig. 1B). The particle size of synthesized SPION@SS-31 was approximately 35.51 ± 0.07 nm (Fig. 1C), which is very close to that of SPION (34.85 ± 1.53 nm). The average zeta potential of SPION@SS-31 was −31.20 ± 3.08 mV (Fig. 1D), a necessary factor in determining the stability of these particles. The differences in physical properties between the SPION and SPION@SS-31 are relatively small which does not affect the application of clinical applications. The above data indicated that SPION@SS-31 exhibits a relatively uniform particle size and good dispersion and stability. The results showed that SS-31 was successfully loaded on SPION to subsequently develop SPION@SS-31. Relative to SPION, the synthesized SPION@SS-31 exhibited similar physical and chemical properties. The course of time showed that SS-31 rapidly released 70 % from SPION@SS-31 at 12 h and almost 90 % at 48 h and continue to 120 h (Fig. 1E).

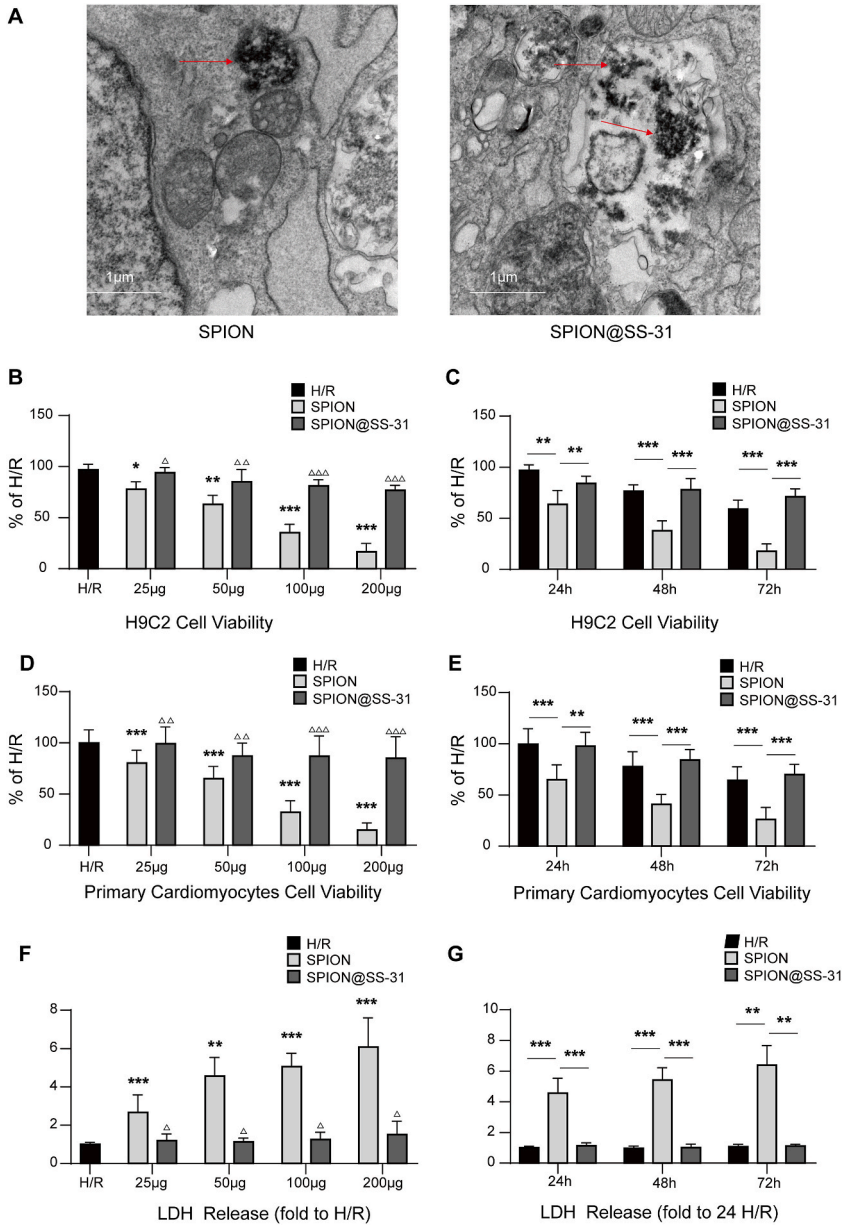

Fig. 2. The internalization and effect of SPION or SPION@SS-31 on the H/R cardiomyocytes viability and injury. (A) TEM images showed the accumulation of iron-containing nanoparticles in cardiomyocytes following incubation with SPION or SPION@SS-31 for 24 h. Red arrows denote the SPION, SPION@SS-31 or particulate matter. (B) Concentration dependent cytotoxic effects of SPION or SPION@SS-31 evaluated after 24 h of incubation by CCK-8 using H9C2 cell line. (C) Time dependent cytotoxic effects of SPION (Fe_3O_4 50 μg/mL) or SPION@SS-31 (Fe_3O_4 50 μg/mL and SS-31 15.82 μg/mL) evaluated after 24 h, 48 h and 72 h of incubation by CCK-8 using H9C2 cell line. (D) Concentration dependent cytotoxic effects of SPION or SPION@SS-31 evaluated after 24 h of incubation by CCK-8 using primary cardiomyocytes. (E) Time dependent cytotoxic effects of SPION (Fe_3O_4 50 μg/mL) or SPION@SS-31 (Fe_3O_4 50 μg/mL and SS-31 15.82 μg/mL) evaluated after 24 h, 48 h and 72 h of incubation by CCK-8 using primary cardiomyocytes. (F) Concentration dependent cell damage of SPION or SPION@SS-31 evaluated after 24 h of incubation by LDH leakage. (G) Time dependent cell damage of SPION or SPION@SS-31 evaluated after 24 h of incubation by LDH leakage. Data were collected from six independent experiments.

(*P < 0.05; **P < 0.01; ***P < 0.001, statistically significant compared to H/R group. △P < 0.05, △△P < 0.01; △△△P < 0.001, statistically significant compared to SPION groups with the same concentration.).

Abbreviations: SPION, superparamagnetic iron oxide nanoparticles; SPION@SS-31, SPION modified with SS-31; H/R, hypoxia/reoxygenation; TEM, transmission electron microscopy; LDH, lactate dehydrogenase.

3.2. SS-31 modification reverses the cytotoxicity induced by SPION

After 24 h of incubation with SPION@SS-31, TEM images revealed the internalization of Fe_3O_4 nanoparticles by H/R cardiomyocytes (Fig. 2A). CCK-8 results demonstrated that H/R cardiomyocytes exposed to SPION exhibited time-dependent as well as concentration-dependent cytotoxicity (Fig. 2B and C). Cell viability tests with primary rat cardiomyocytes also show same trends. With increasing concentrations of SPION (25, 50, 100, 200 μg/mL), the percent viability was decreased from 77.7 % to 16.5 % after 24 h (Fig. 2D). At a 50 μg/mL concentration, the viability of cells at 24, 48 and 72 h was 63.7 %, 37.8 % and 17.7 %, respectively (Fig. 2E). Interestingly, SS-31 significantly mitigated the time- and concentration-dependent cytotoxicity of SPION, as evidenced by the comparable cell viability between H/R and SPION@SS-31 groups (all $p > 0.05$). Additionally, compared to H/R H9C2 cells, the group treated with SPION exhibited markedly increased LDH release in concentration-dependent and time-dependent manner, while LDH activities did not exhibit a considerable difference between the H/R groups and the SPION@SS-31 group (Fig. 2F and G). These results indicated SS-31 modification may remarkably inhibit SPION-induced cell damage by releasing SS-31 from SPION@SS-31.

3.3. SS-31 modification alleviates oxidative stress induced by SPION

The generation of mitochondrial ROS from SPION was detected using MitoSOX staining. As indicated in Fig. 3A-3B, SPION demonstrated dramatically higher levels of mitochondrial ROS than SPION@SS-31. Notably, in the SPION@SS-31 group, generation of mitochondrial ROS levels were similar to the H/R group ($p > 0.05$), suggesting that SS-31 modification effectively reverses SPION-induced cellular oxidative stress. We further detected the levels of GSH and GPX4, which not only reflect the antioxidant capacity of cells but are also Ferroptosis markers. The SPION group showed a notable reduction in both GSH and GPX4 activity compared to the SPION@SS-31 group (Fig. 3C–D). Again, no remarkable differences were found between SPION@SS-31 and H/R groups, suggesting that the SS-31 modification could effectively correct the imbalance of oxidation and antioxidation caused by SPION.

3.4. SS-31 modification rescues mitochondrial function and structure damaged by SPION

We next investigated the function and morphology of mitochondria among the three groups. As illustrated in Fig. 4, the SPION

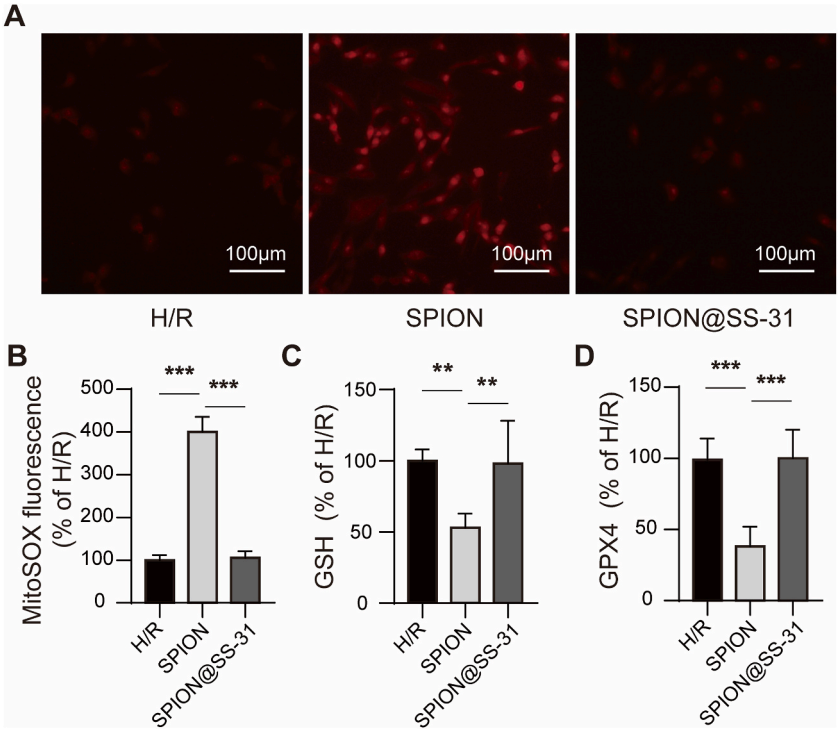

Fig. 3. Effects on mitochondrial ROS and antioxidant capacity in H/R cardiomyocytes treated with SPION (Fe_3O_4 50 μg/mL) or SPION@SS-31 (Fe_3O_4 50 μg/mL and SS-31 15.82 μg/mL) for 24 h. (A) Representative photomicrographs of mitochondrial ROS in H/R cardiomyocytes visualized by fluorescent microscopy. Red fluorescent intensity indicated ROS accumulation. (B) Quantitative analysis of red fluorescent intensity in individual group. (C–D) The concentrations of GSH and GPX4 were measured by ELISA. Data were collected from six independent experiments. (**$P < 0.01$; ***$P < 0.001$.).

Abbreviations: SPION, superparamagnetic iron oxide nanoparticles; SPION@SS-31, SPION modified with SS-31; H/R, hypoxia/reoxygenation; ROS, reactive oxygen species; GSH, glutathione; GPX4, glutathione peroxidase 4; ELISA, enzyme-linked immunosorbent assay.

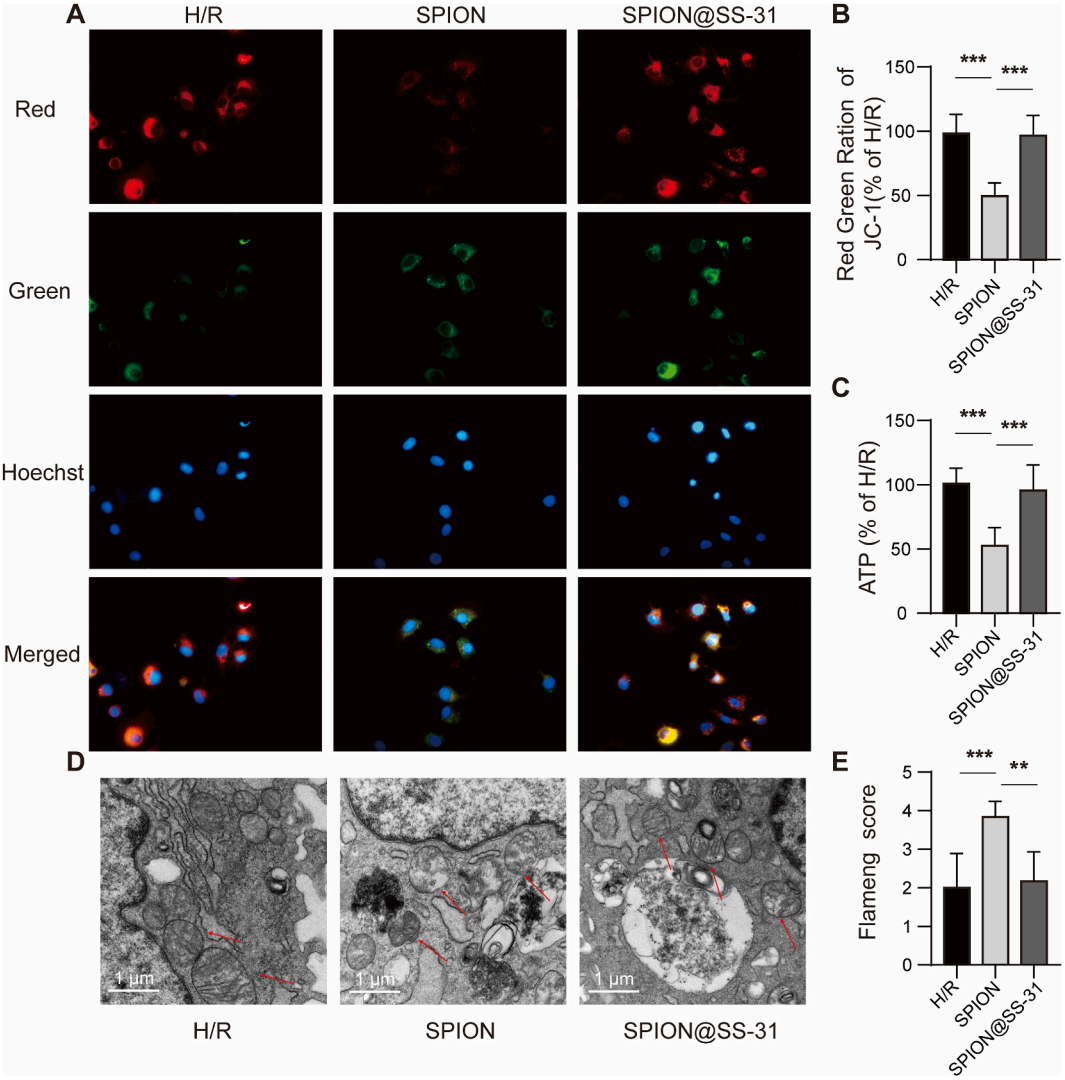

Fig. 4. Effects on structure and function changes of mitochondria of H/R cardiomyocytes treated with SPION (Fe_3O_4 50 μg/mL) or SPION@SS-31 (Fe_3O_4 50 μg/mL and SS-31 15.82 μg/mL) for 24 h. (A) MMP was assessed by fluorescence microscopy with JC-1 staining. (B) Quantitative analysis of MMP by plate reader. (C) The level of ATP was measured by ELISA. (D–E) Representative TEM images and corresponding relative Flameng scores obtained from H/R cardiomyocytes treated with SPION or SPION@SS-31. Data were collected from six independent experiments. (**P < 0.01; ***P < 0.001.)

Abbreviations: SPION, superparamagnetic iron oxide nanoparticles; SPION@SS-31, SPION modified with SS-31; H/R, hypoxia/reoxygenation; MMP, Mitochondrial membrane potential; ATP, adenosine-triphosphate; ELISA, enzyme-linked immunosorbent assay; TEM, transmission electron microscopy.

group showed a marked loss of MMP (Fig. 4A–B) and severe ATP depletion (Fig. 4C) when compared to the H/R group. Interestingly, in the SPION@SS-31 group, both MMP and ATP levels were comparable to the H/R group ($p > 0.05$), indicating that SS-31 modification could maintain relatively stable mitochondrial function. TEM images revealed severely distorted and enlarged mitochondria in the SPION group, whereas the changes in mitochondria between SPION@SS-31 and H/R group were similar, characterized by mildly swollen mitochondria and relatively intact mitochondrial cristae (Fig. 4D). Furthermore, mitochondrial damage, as assessed using the Flameng score [26], the score in the SPION group was 1.76 times higher than in the SPION@SS-31 group (Fig. 4E). This lack of difference between the SPION@SS-31 and H/R groups implie that SS-31 modification can effectively protect mitochondria from SPION-induced oxidative attack. Taken together, the above results suggested that SPION could seriously damage mitochondria, but the detrimental effects could be alleviated by SS-31 release from SPION@SS-31.

3.5. SS-31 modification inhibits ferroptosis driven by SPION by protecting mitochondria

To explore the effects of Fe_3O_4 nanoparticles (SPION or SPION@SS-31) on cell iron metabolism, we detected a series of iron

metabolism-related proteins and the level of nonheme iron. WB analysis demonstrated that the expression of ferritin H was significantly upregulated in both the SPION and SPION@SS-31 groups compared to the H/R group (Fig. 5A–B), accompanied by marked downregulation of TfR1 in the SPION and SPION@SS-31 groups (Fig. 5C–D). Notably, the expression of cellular iron export protein (FPN1) and mitochondrial iron export protein (ABCB8) also dramatically decreased both in the SPION and SPION@SS-31 groups (Fig. 6A–D). These results indicated that both SPION and SPION@SS-31 induce an imbalance in cellular iron metabolism, as evidenced by the increase in stored iron and the decrease in iron efflux. Nonheme iron levels were also significantly elevated in both the cytoplasm and mitochondria of the SPION and SPION@SS-31 groups, especially in the mitochondria (Fig. 7A–B), especially in mitochondria, suggesting that both SPION and SPION@SS-31 induced mitochondrial iron overload. ELISA detection showed that FtMt in the SPION@SS-31 and SPION groups was at least 4 times higher than the H/R group, supporting the notion that both SPION and SPION@SS-31 mainly induced iron overload in mitochondria in H/R cardiomyocytes (Fig. 7C).

Next, we tested the lipid peroxidation product MDA in the cytoplasm and mitochondria. The SPION and SPION@SS-31 groups exhibited higher cytosolic MDA levels compared to the H/R group (Fig. 7D). Interestingly, mitochondrial MDA levels were lower in the SPION@SS-31 group than in the SPION group (Fig. 7E), with no remarkable difference between the SPION@SS-31 and H/R groups, indicating that SS-31 may protect mitochondria from oxidative stress through its targeted antioxidant action.

To further assess whether SPION could lead to ferroptotic cell death by inducing mitochondrial iron overload, we detected molecular markers of Ferroptosis. The SPION group displayed higher levels of NRF2, GPX4, and ACSL4 compared to the H/R group (Fig. 8A–F), while the SPION@SS-31 group had similar expression levels to the H/R group ($p > 0.05$). Additionally, the mRNA levels of ACSL4 and Ptgs2 were significantly elevated in the SPION group compared to the H/R group, but not in the SPION@SS-31 group (Fig. 8G–H). Notably, the SPION@SS-31 group exhibited similar mRNA levels of ACSL4 and Ptgs2 in H/R group (both $p > 0.05$). These results clearly suggest that SPION could cause Ferroptosis by aggravating the iron load of mitochondria to promote a lipid peroxidation burst in H/R cardiomyocytes.

To determine whether ferroptosis is the primary cause of SPION-induced cell death, we treated H/R cardiomyocytes with SPION, SPION@SS-31, and various cell death inhibitors, including Fer-1 (ferroptosis inhibitor), 3-MA (autophagy inhibitor), Nec-1 (necroptosis inhibitor), and zVAD (apoptosis inhibitor) for 24 h. As shown in Fig. 8I, SPION-induced cell viability loss was reversed by Fer-1 but could not be inhibited by 3-MA, Nec-1, or zVAD, indicating that Ferroptosis is probably the main death form of cardiomyocytes mediated by SPION. Interestingly, cardiomyocytes treated with SPION@SS-31 exhibited cell viability similar to that of cardiomyocytes treated with Fer-1 ($p > 0.05$), suggesting that SS-31 significantly inhibits SPION-induced ferroptosis.

Taken together, these results suggest that SPION promotes ferroptosis in H/R cardiomyocytes by inducing mitochondrial iron overload, which lead to lipid peroxidation burst. However, SS-31 effectively mitigates these adverse effects by preventing mitochondrial oxidative damage triggered by SPION.

4. Limitation

The findings of this study have some limitations. First, different iron oxide nanoparticles types and coatings may exhibit varying toxicities, requiring further detailed investigation. Second, our research was limited to in vitro cellular experiments, and the protective effects of SS-31 in vivo remain uncertain. In vivo validation is necessary for the findings from in vitro assays. Third, we observed a

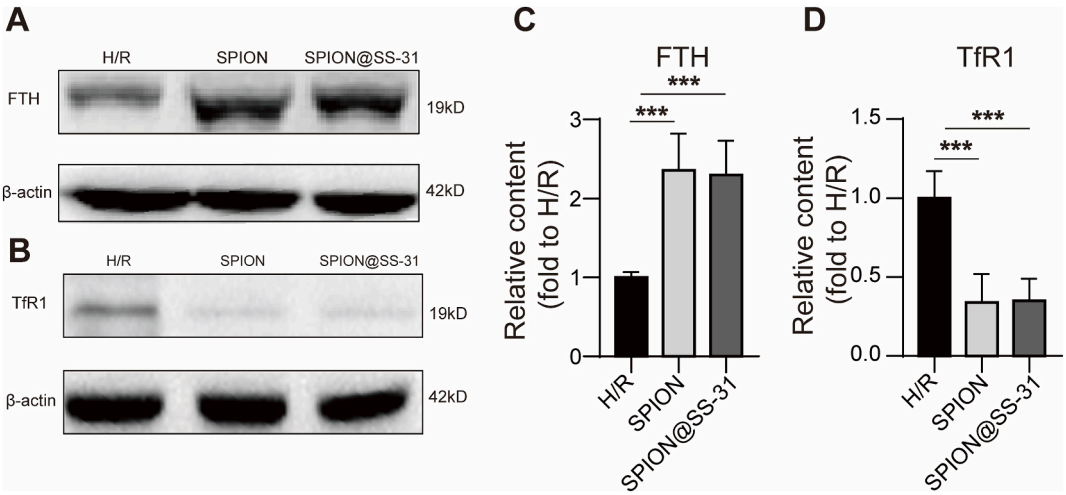

Fig. 5. Expression of iron storage related proteins induced by SPION (Fe_3O_4 50 μg/mL) or SPION@SS-31 (Fe_3O_4 50 μg/mL and SS-31 15.82 μg/mL). (A and C) FTH and TfR1 determined by WB in H/R cardiomyocytes exposed to SPION or SPION@SS-31 for 24 h. (B and D) Quantitative analysis of FTH and TfR1 using data from six independent experiments. (**P < 0.01; ***P < 0.001.) Full WB image can be found in Supplementary Material. Abbreviations: SPION, superparamagnetic iron oxide nanoparticles; SPION@SS-31, SPION modified with SS-31; H/R, hypoxia/reoxygenation; FTH, ferritin H; TfR1, transferrin receptor 1; WB, western blotting.

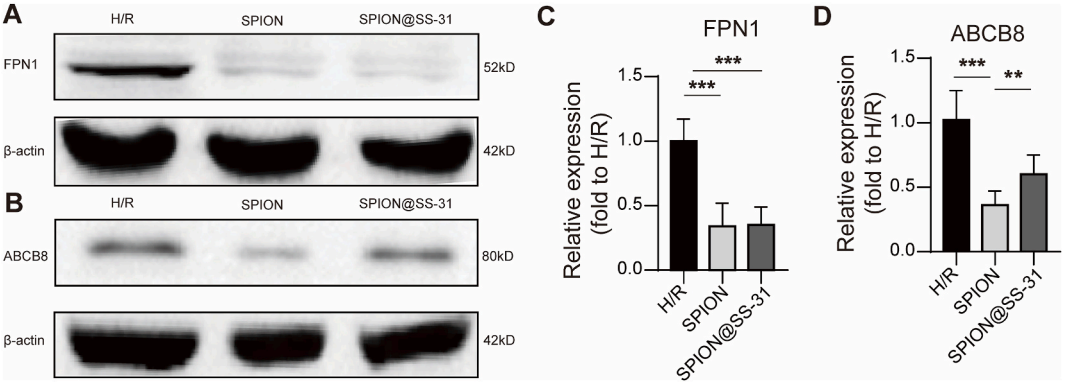

Fig. 6. Expression of iron efflux related proteins induced by SPION (Fe_3O_4 50 μg/mL) or SPION@SS-31 (Fe_3O_4 50 μg/mL and SS-31 15.82 μg/mL). (A and C) FPN1 and ABCB8 determined by WB in H/R cardiomyocytes exposed to SPION or SPION@SS-31 for 24 h. (B and D) Quantitative analysis of FPN1 and ABCB8 using data from six independent experiments. (**P < 0.01; ***P < 0.001.) Full WB image can be found in Supplementary Material.

Abbreviations: SPION, superparamagnetic iron oxide nanoparticles; SPION@SS-31, SPION modified with SS-31; H/R, hypoxia/reoxygenation; FPN1, ferroportin1; ABCB8, ATP binding cassette protein B8; WB, western blotting.

trend suggesting that SPION may contribute to increased cell viability loss in H/R cardiomyocytes after 24 h of exposure. Given that previous studies have confirmed the concentration- and time-dependent cytotoxicity of iron oxide, our findings could be influenced by the short observation period (24 h) and the relatively low concentration of SPION (50 μg Fe_3O_4). Higher concentrations and longer exposure times are necessary to further elucidate the toxicity of SPION and the antioxidant effects of SS-31. Therefore, future studies should explore the chronic toxic effects and determine if SPION@SS-31 can provide long-term protection in vivo.

5. Discussion

This study is the first to reveal that SPIONs significantly increase mitochondrial iron load in H/R cardiomyocytes, triggering ferroptosis by inducing lipid peroxidation, which damages mitochondria. The SS-31 was found to significantly mitigate SPION-induced Ferroptosis in cardiomyocytes by protecting mitochondria. The results suggest that modifying SPION with SS-31 could be a promising approach to mitigate myocardial toxicity caused by SPION.

A thorough understanding of the cytotoxic mechanisms of SPION is crucial to enhance their safety. Recent studies have revealed that Fe_3O_4 nanoparticles can promote Ferroptosis in tumor cells by accelerating the Fenton reaction [27,28], or enhancing autophagy-dependent Ferroptosis pathway [29], which has been used to inhibit tumor growth. Our previous work revealed that SPION exacerbates oxidative stress in H/R cardio myocardium in vitro [8]. The present study showed that SPION can drive Ferroptosis by inducing mitochondrial iron overload in H/R cardiomyocytes. Ferroptosis is a new form of regulated the death of cell, driven by iron-dependent lipid peroxidation, and differs from apoptosis, necroptosis, and autophagy in its morphology, biochemistry, and genetics [30]. It has been recognized as a key contributor to the injury of I/R in organs such as the heart, brain, and kidneys [31,32].

Recent studies have reported that doxorubicin (DOX) and cardiac I/R can lead to mitochondrial iron overload in cardiomyocytes [11,33], promoting mitochondrial membrane lipid peroxidation to cause Ferroptosis of cardiomyocytes [11]. Additionally, increased cardiac non-heme iron, along with reduced levels of mt-Cytb and mt-Atp6 mRNA, facilitate the Ferroptosis of cardiomyocytes to result in left ventricular negative remodeling in mouse myocardial I/R model. Treatments with Fer-1 or the iron chelator dexrazoxane could significantly improve the detrimental outcome [11], not only implying Ferroptosis is a critical part of the pathological process of myocardial I/R injury but also suggesting that mitochondria may be important organelles affecting Ferroptosis in cardiomyocytes.

Our previous study demonstrated that co-loading the antioxidant N-acetylcysteine (NAC) can mitigate the SPION-induced toxicity in H/R cardiomyocytes [8]. However, NAC was ineffective in preventing negative left ventricular remodeling after myocardial I/R in rats, likely due to mitochondrial iron overload, decrease in GSH and GPX4 activity, and lipid peroxidation (unpublished data). We speculate that mitochondria may be the primary organelle targeted by SPION, with SPION exacerbating Ferroptosis in I/R cardiomyocytes by inducing iron overload and lipid peroxidation in mitochondria. As NAC is an untargeted antioxidant, it did not provide the targeted antioxidant protection needed for mitochondria. For this reason, we hypothesized that mitochondrial-targeted antioxidant peptides could potentially alleviate the myocardial toxicity of SPION.

Among the SS polypeptides, SS-31 has emerged as the most effective agent for protecting against I/R injury [17,34]. Upon entering the mitochondria, SS-31 scavenges reactive oxygen species by forming inactive tyrosyl groups, reducing lipid peroxidation and cardiomyocyte death, and limiting myocardial infarct size [35,36]. Additionally, a phase 2a trial assessing the efficacy and safety of Elamipretide (SS-31) in primary percutaneous coronary intervention patients, confirmed SS-31's safety and tolerability [37]. Based on these findings, we modified SPION with SS-31 by a physical adsorption method to develop SPION@SS-31. Compared with the SPION group, SPION@SS-31 remarkably decreased the level of mitochondrial MDA and preserved the levels of GSH and GPX4, while there was no significant difference between the SPION@SS-31 and H/R groups. Moreover, the SPION@SS-31 group exhibited notably lower

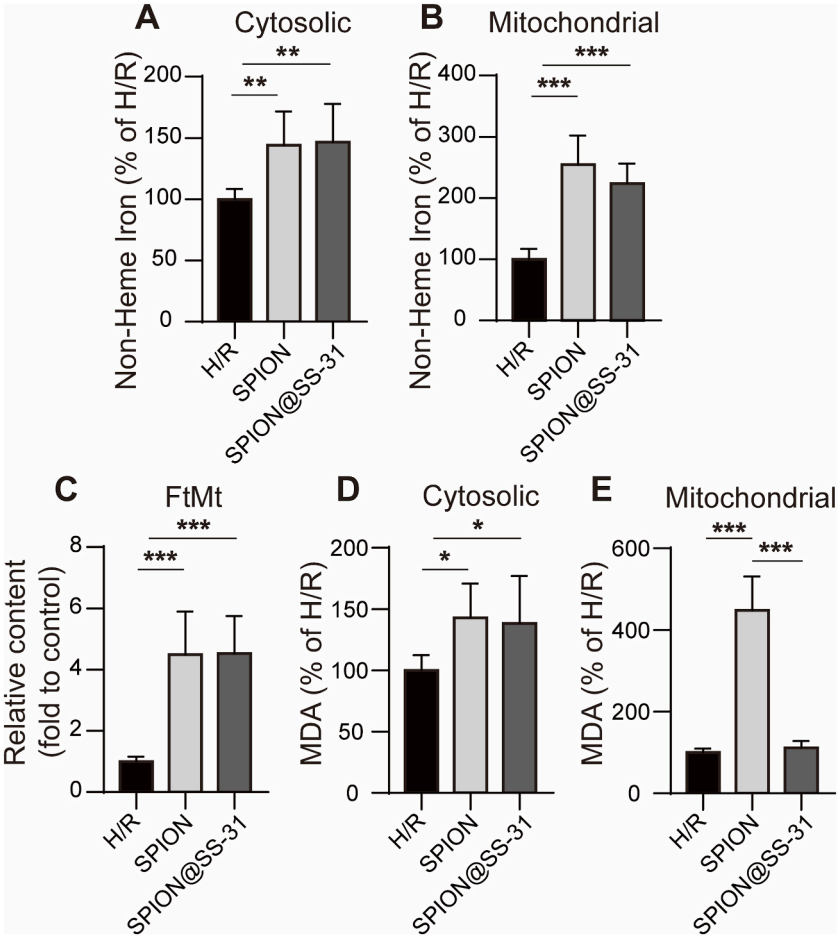

Fig. 7. Effects on cellular iron load and lipid peroxidation induced by SPION (Fe_3O_4 50 μg/mL) or SPION@SS-31 (Fe_3O_4 50 μg/mL and SS-31 15.82 μg/mL). (A–B) Cytosolic and mitochondrial nonheme iron were measured in H/R cardiomyocytes treated with SPION or SPION@SS-31 for 24 h. (C) The levels of FtMt were detected in H/R cardiomyocytes treated with SPION or SPION@SS-31 for 24 h. (D–E) Cytosolic and mitochondrial MDA levels were measured in H/R cardiomyocytes treated with SPION or SPION@SS-31 for 24 h. Data were collected from six independent experiments. (*P < 0.05; **P < 0.01; ***P < 0.001.)

Abbreviations: SPION, superparamagnetic iron oxide nanoparticles; SPION@SS-31, SPION modified with SS-31; H/R, hypoxia/reoxygenation; FtMt, mitochondrial ferritin; MDA, malonaldehyde.

expression of NRF2 and ACSL4 and higher GPX4 levels compared to the SPION group. While mRNA levels of Ptgs2 and ACSL4 were also remarkably reduced in the SPION@SS-31 group. Furthermore, there was no remarkably difference between the SPION@SS-31 and H/R groups, suggesting that SS-31 can effectively rescue mitochondrial lipid peroxidation and subsequent Ferroptosis mediated by SPION.

Both SPION and SPION@SS-31 induced an imbalance in iron metabolism in H/R cardiomyocytes, characterized by an excessive iron load in mitochondria. SS-31, as a mitochondrial targeted antioxidant peptide, has no significant effect on iron metabolism in cells, which is consistent with its inability to chelate iron. Notably, the cells in SPION@SS-31 group express higher ABCB8 than in the SPION group, implying the cardiomyocytes exposed to SPION@SS-31 may have the potential to maintain mitochondrial iron homeostasis to some extent. This result may be attributed to the possibility that SS-31 effectively protected mitochondria from ROS attack to maintain iron metabolic homeostasis.

To confirm Ferroptosis as the primary mode of SPION-induced cardiomyocyte death, we treated H/R cardiomyocytes with 3-MA, Nec-1, zVAD, or Fer-1. Only Fer-1 rescued cell viability, indicating that Ferroptosis is likely the primary mechanism of SPION-induced cardiotoxicity. Interestingly, SS-31 demonstrated similar protective effects to Fer-1, implying that SS-31 modification could significantly inhibit SPION-induced Ferroptosis by protecting the mitochondria. The results need to be further verified by animal experiments.

What should be considered is that animal experiments are inherently more complex than in vitro studies. First, in vitro, cardiomyocytes have a limited capacity to phagocytize and degrade SPION, resulting in relatively low concentrations of free iron released from SPION. However, in the ischemic myocardium, SPION application leads to the recruitment of a significant number of macrophages to the peri-infarct zones. These macrophages engulf and degrade SPION, which likely becomes the primary degradation

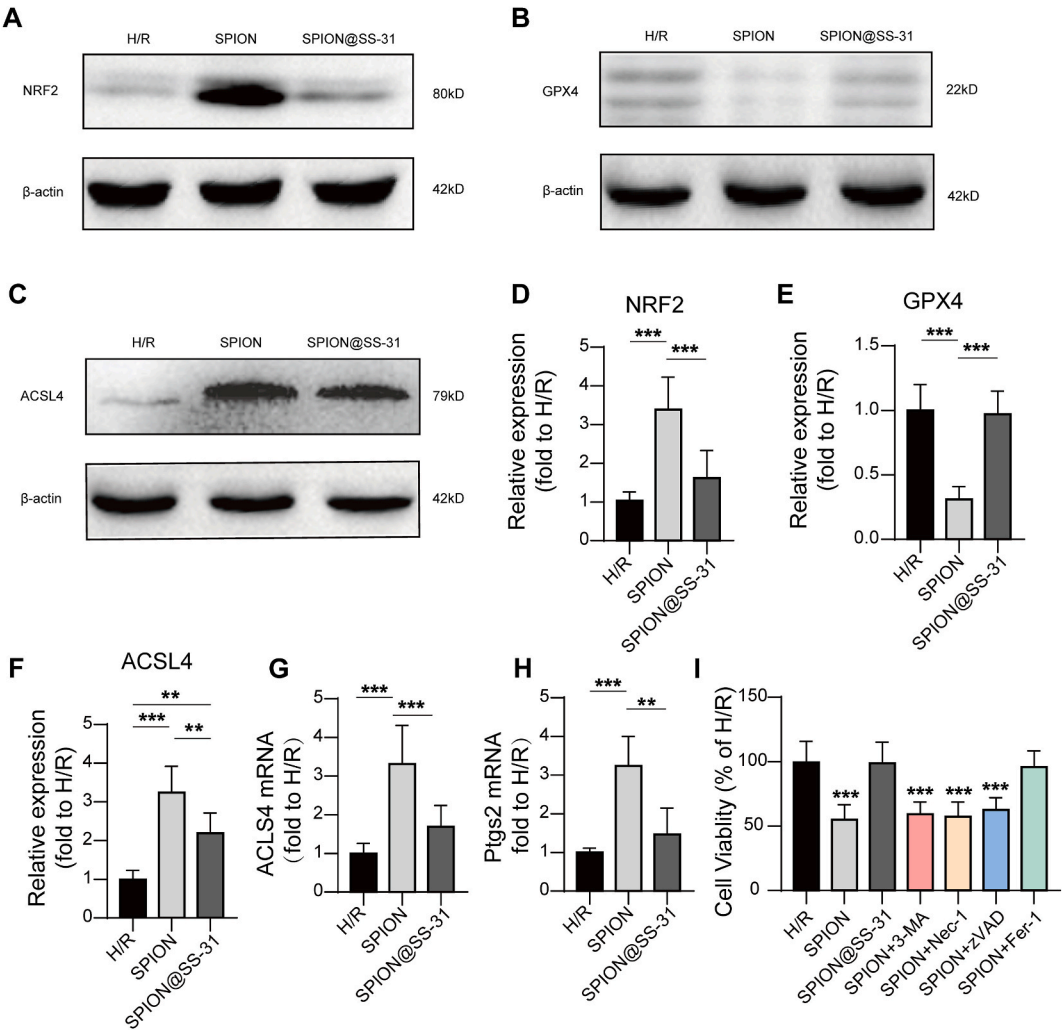

Fig. 8. Effects of SPION (Fe_3O_4 50 μg/mL) or SPION@SS-31 (Fe_3O_4 50 μg/mL and SS-31 15.82 μg/mL) on ferroptosis in H/R cardiomyocytes. (A, B and C) NFR2, GPX4 and ACSL4 determined by WB in H/R cardiomyocytes exposed to SPION or SPION@SS-31 for 24 h. Full WB image can be found in Supplementary Material. (D, E and F) Quantitative analysis of NFR2, GPX4 and ACSL4 by WB. (G and H) Relative levels of ACSL4 mRNA and Ptgs2 mRNA were measured in H/R cardiomyocytes exposed to SPION or SPION@SS-31 for 24 h. (I) Effects of different cell death inhibitors on viability of H/R cardiomyocytes exposed to SPION. Data were collected from six independent experiments.
(**P < 0.01; ***P < 0.001.).
Abbreviations: SPION, superparamagnetic iron oxide nanoparticles; SPION@SS-31, SPION modified with SS-31; H/R, hypoxia/reoxygenation; NFR2, nuclear erythroid factor 2; GPX4, glutathione peroxidase 4; ACSL4, long-chain acyl-CoA synthetase; Ptgs2, prostaglandin-endoperoxide synthase 2; WB, western blotting.

pathway in myocardial tissue, potentially causing more severe mitochondrial iron overload and Ferroptosis. Second, iron oxide nanoparticles have been shown to promote pro-inflammatory macrophage polarization, which may pose an additional risk in ischemic myocardium following myocardial infarction [38,39]. These suggest that SPION application in ischemic myocardium may increase the risk of inflammatory reactions following myocardial infarction. Our in vitro study demonstrated that SS-31 modification inhibits SPION-induced pro-inflammatory effects in macrophages [40]. Further research is aimed to determine whether the anti-inflammatory effects of SS-31 on SPION can be further confirmed in vivo. Third, since ultra-small SPION has been shown to induce Ferroptosis in a time-dependent manner in human breast cancer cells [41], indicating that the sustained release of SPION@SS-31 is crucial for maintaining a continuously sufficient concentration of SS-31 in vivo studies. In our future research, we aim to elucidate the interactions between macrophages and SPION when applied to ischemic myocardium. The exploration of SPION-related Ferroptosis mechanisms will involve an increased utilization of primary cardiomyocytes and animal experiments in our future studies.

6. Conclusions

SS-31 modification could significantly reduce SPION-induced H/R cardiomyocytes Ferroptosis by preventing mitochondrial oxidative damage in vitro, suggesting a hopeful approach to decrease the myocardial toxicity of SPION.

Funding

This research was supported by the National Natural Science Foundation of China [grant numbers 52071194 and 82070365]; the Top-level Clinical Discipline Project of Shanghai Pudong New Area, China [grant number PWYgf 2021-01]; the Health Science and Technology Project of Shanghai Pudong New Area Health Commission, China [grant number PW2019A-13] and the Training plan for discipline leaders of Shanghai Pudong New Area Health Commission, China [grant number PWRd2020-09].

Data availability statement

The data that support the findings of this study are available from the corresponding author upon reasonable request.

Ethics declarations

The study complies with all ethics regulations.

Animal experiments were conducted with the approval of the Animal Care and Use Committee of Tongji University, in accordance with the Guide for the Care and Use of Laboratory Animals, from National Academy Press (NIH Publication No. 85-23, revised 1996).

CRediT authorship contribution statement

Qizheng Lu: Writing – review & editing, Writing – original draft, Supervision, Project administration, Methodology, Investigation, Formal analysis, Conceptualization. **Xiaobo Yao:** Writing – original draft, Methodology, Investigation. **Hao Zheng:** Writing – original draft, Methodology, Investigation. **Jinbo Ou:** Formal analysis, Data curation. **Jieyun You:** Writing – review & editing, Formal analysis. **Qi Zhang:** Writing – review & editing, Supervision. **Wei Guo:** Writing – review & editing, Supervision. **Jing Xu:** Writing – review & editing, Formal analysis. **Li Geng:** Data curation. **Qinghua Liu:** Writing – review & editing. **Ning Pei:** Writing – review & editing. **Yongyong Gong:** Data curation, Conceptualization. **Hongming Zhu:** Writing – review & editing, Supervision, Conceptualization. **Yunli Shen:** Writing – review & editing, Writing – original draft, Supervision, Project administration, Methodology, Investigation, Formal analysis, Conceptualization.

Declaration of competing interest

The authors declare that they have no known competing financial interests or personal relationships that could have appeared to influence the work reported in this paper.

Appendix A. Supplementary data

Supplementary data to this article can be found online at https://doi.org/10.1016/j.heliyon.2024.e38584.

References

[1] C.J. Murphy, G.Y. Oudit, Iron-overload cardiomyopathy: pathophysiology, diagnosis, and treatment, J. Card. Fail. 16 (11) (2010) 888–900.
[2] A. Avasthi, et al., Magnetic nanoparticles as MRI contrast agents, Top. Curr. Chem. 378 (3) (2020) 40.
[3] A.B. Mathiasen, et al., In vivo MRI tracking of mesenchymal stromal cells labeled with ultrasmall paramagnetic iron oxide particles after intramyocardial transplantation in patients with chronic ischemic heart disease, Stem Cell. Int. 2019 (2019) 2754927.
[4] Z. Huang, et al., The effect of nonuniform magnetic targeting of intracoronary-delivering mesenchymal stem cells on coronary embolisation, Biomaterials 34 (38) (2013) 9905–9916.
[5] H. Yang, et al., Engineering human ventricular heart tissue based on macroporous iron oxide scaffolds, Acta Biomater. 88 (2019) 540–553.
[6] A. Nemmar, et al., Ultrasmall superparamagnetic iron oxide nanoparticles acutely promote thrombosis and cardiac oxidative stress and DNA damage in mice, Part. Fibre Toxicol. 13 (1) (2016) 22.
[7] V. Manickam, et al., Recurrent exposure to ferric oxide nanoparticles alters myocardial oxidative stress, apoptosis and necrotic markers in male mice, Chem. Biol. Interact. 278 (2017) 54–64.
[8] Y. Shen, et al., Co-loading antioxidant N-acetylcysteine attenuates cytotoxicity of iron oxide nanoparticles in hypoxia/reoxygenation cardiomyocytes, Int. J. Nanomed. 14 (2019) 6103–6115.
[9] W. Cai, et al., Alox15/15-HpETE aggravates myocardial ischemia-reperfusion injury by promoting cardiomyocyte ferroptosis, Circulation 147 (19) (2023) 1444–1460.
[10] Y. Chen, et al., Ferroptosis: a novel therapeutic target for ischemia-reperfusion injury, Front. Cell Dev. Biol. 9 (2021) 688605.
[11] X. Fang, et al., Ferroptosis as a target for protection against cardiomyopathy, Proc. Natl. Acad. Sci. U. S. A. 116 (7) (2019) 2672–2680.
[12] Y. Huang, et al., Superparamagnetic iron oxide nanoparticles induce ferroptosis of human ovarian cancer stem cells by weakening cellular autophagy, J. Biomed. Nanotechnol. 16 (11) (2020) 1612–1622.

[13] J. Wen, et al., Ultrasmall iron oxide nanoparticles induced ferroptosis via Beclin1/ATG5-dependent autophagy pathway, Nano Converg 8 (1) (2021) 10.
[14] Y. Li, et al., The potential application of nanomaterials for ferroptosis-based cancer therapy, Biomed. Mater. 16 (4) (2021).
[15] H. Zheng, et al., Superparamagnetic iron oxide nanoparticles promote ferroptosis of ischemic cardiomyocytes, J. Cell Mol. Med. 24 (18) (2020) 11030–11033.
[16] Q. Peng, et al., ROS-independent toxicity of Fe3O4 nanoparticles to yeast cells: involvement of mitochondrial dysfunction, Chem. Biol. Interact. 287 (2018) 20–26.
[17] J. Cai, et al., Protective effects of mitochondrion-targeted peptide SS-31 against hind limb ischemia-reperfusion injury, J. Physiol. Biochem. 74 (2) (2018) 335–343.
[18] L. Shang, et al., SS-31 protects liver from ischemia-reperfusion injury via modulating macrophage polarization, Oxid. Med. Cell. Longev. 2021 (2021) 6662156.
[19] T. Imai, et al., The mitochondria-targeted peptide, Bendavia, attenuated ischemia/reperfusion-induced stroke damage, Neuroscience 443 (2020) 110–119.
[20] F.Y. Lee, et al., Combined therapy with SS31 and mitochondria mitigates myocardial ischemia-reperfusion injury in rats, Int. J. Mol. Sci. 19 (9) (2018).
[21] A. Gallo-Cordova, S. Veintemillas-Verdaguer, Engineering iron oxide nanocatalysts by a microwave-assisted polyol method for the magnetically induced degradation of organic pollutants 11 (4) (2021).
[22] W.Y. Wu, et al., The natural flavone acacetin confers cardiomyocyte protection against hypoxia/reoxygenation injury via AMPK-mediated activation of Nrf2 signaling pathway, Front. Pharmacol. 9 (2018) 497.
[23] H. Towbin, T. Staehelin, J. Gordon, Electrophoretic transfer of proteins from polyacrylamide gels to nitrocellulose sheets: procedure and some applications, Proc. Natl. Acad. Sci. U. S. A. 76 (9) (1979) 4350–4354.
[24] Y. Xin, et al., Manganese transporter Slc39a14 deficiency revealed its key role in maintaining manganese homeostasis in mice, Cell Discov 3 (2017) 17025.
[25] J.H. Lin, et al., Xanthohumol protects the rat myocardium against ischemia/reperfusion injury-induced ferroptosis, Oxid. Med. Cell. Longev. 2022 (2022) 9523491.
[26] W. Flameng, et al., Ultrastructural and cytochemical correlates of myocardial protection by cardiac hypothermia in man, J. Thorac. Cardiovasc. Surg. 79 (3) (1980) 413–424.
[27] M. Sang, et al., Mitochondrial membrane anchored photosensitive nano-device for lipid hydroperoxides burst and inducing ferroptosis to surmount therapy-resistant cancer, Theranostics 9 (21) (2019) 6209–6223.
[28] Z. Shen, et al., Fenton-reaction-acceleratable magnetic nanoparticles for ferroptosis therapy of orthotopic brain tumors, ACS Nano 12 (11) (2018) 11355–11365.
[29] H. Chen, J. Wen, Iron oxide nanoparticles loaded with paclitaxel inhibits glioblastoma by enhancing autophagy-dependent ferroptosis pathway, Eur. J. Pharmacol. 921 (2022) 174860.
[30] S.J. Dixon, et al., Ferroptosis: an iron-dependent form of nonapoptotic cell death, Cell 149 (5) (2012) 1060–1072.
[31] X. Li, et al., Targeting ferroptosis: pathological mechanism and treatment of ischemia-reperfusion injury, Oxid. Med. Cell. Longev. 2021 (2021) 1587922.
[32] H.F. Yan, et al., The pathological role of ferroptosis in ischemia/reperfusion-related injury, Zool. Res. 41 (3) (2020) 220–230.
[33] Y. Ichikawa, et al., Cardiotoxicity of doxorubicin is mediated through mitochondrial iron accumulation, J. Clin. Invest. 124 (2) (2014) 617–630.
[34] A. Saad, et al., Phase 2a clinical trial of mitochondrial protection (Elamipretide) during stent revascularization in patients with atherosclerotic renal artery stenosis, Circ Cardiovasc Interv 10 (9) (2017).
[35] W. Dai, et al., Bendavia, a mitochondria-targeting peptide, improves postinfarction cardiac function, prevents adverse left ventricular remodeling, and restores mitochondria-related gene expression in rats, J. Cardiovasc. Pharmacol. 64 (6) (2014) 543–553.
[36] J. Shi, et al., Bendavia restores mitochondrial energy metabolism gene expression and suppresses cardiac fibrosis in the border zone of the infarcted heart, Life Sci. 141 (2015) 170–178.
[37] C.M. Gibson, et al., EMBRACE STEMI study: a Phase 2a trial to evaluate the safety, tolerability, and efficacy of intravenous MTP-131 on reperfusion injury in patients undergoing primary percutaneous coronary intervention, Eur. Heart J. 37 (16) (2016) 1296–1303.
[38] S. Zanganeh, et al., Iron oxide nanoparticles inhibit tumour growth by inducing pro-inflammatory macrophage polarization in tumour tissues, Nat. Nanotechnol. 11 (11) (2016) 986–994.
[39] W. Zhang, et al., Differently charged super-paramagnetic iron oxide nanoparticles preferentially induced M1-like phenotype of macrophages, Front. Bioeng. Biotechnol. 8 (2020) 537.
[40] Q.Z. Lu, et al., SS-31 modification inhibits the proinflammatory effect on macrophages induced by superparamagnetic iron oxide nanoparticles, J. Biomed. Nanotechnol. 18 (5) (2022) 1413–1422.
[41] J. Gao, et al., Time-course effect of ultrasmall superparamagnetic iron oxide nanoparticles on intracellular iron metabolism and ferroptosis activation, Nanotoxicology 15 (3) (2021) 366–379.